LETTER

Nanofibers Doped with Dendritic Fluorophores for Protein Detection

Bryce W. Davis,[†] Nakorn Niamnont,[‡] Christopher D. Hare,[†] Mongkol Sukwattanasinitt,[*,‡] and Quan Cheng[*,†]

Department of Chemistry, University of California, Riverside, California 92521, Organic Synthesis Research Unit, Department of Chemistry, Faculty of Science, and Center for Petroleum, Petrochemicals and Advanced Materials, Chulalongkorn University, Bangkok 10330, Thailand

ABSTRACT We report a solid-state, nanofiber-based optical sensor for detecting proteins with an anionic fluorescent dendrimer (AFD). The AFD was encapsulated in cellulose acetate (CA) electrospun nanofibers, which were deacetylated to cellulose to generate secondary porous structures that are desirable for enhancing molecular interactions, and thus better signaling. The protein sensing properties of the fibers were characterized by monitoring the fluorescence response of cytochrome c (cyt c), hemoglobin (Hgb), and bovine serum albumin (BSA) as a function of concentration. Effective quenching was observed for the metalloproteins, cyt c and Hgb. The effect was primarily due to energy transfer of the imbedded fluorescent dendrimers to the protein, as both proteins contain heme portions. Electron transfer, caused through the electrostatic effects in the binding of the anionic dendrimer to the positive patches of globular proteins, could be responsible as well. BSA, on the other hand, triggered a "turn-on" response in fluorescence, suggesting the negatively charged BSA reduces the $\pi-\pi$ stacking of the partially dispersed, negatively charged dendritic fluorophores through repulsion forces, which results in an increase in fluorescence. Stern−Volmer constants (K_{sv}) of the electrospun fibers were found to be 3.4×10^5 and 1.7×10^6 M^{-1} for cyt c and Hgb, respectively. The reusability of the nanofibers is excellent: the nanofibers demonstrated less than 15% change of fluorescence intensity signal in a 5-cycle test.

KEYWORDS: electrospinning • fluorescent dendrimers • protein biosensor • nanofibers

1. INTRODUCTION

The development of solid-state optical biosensors continues to be of major interest within the nanotechnology field because of many practical and potential functions (1). For instance, these solid-state sensors can exhibit advantages of versatility, sensitivity, selectivity, simplified optical setup, and a large dynamic range. However, desirable mechanical, electronic, and optical properties can be difficult to realize at the sensing interface because they require sophisticated synthesis routes and tend to use a broad range of discontinuous objects such as carbon nanotubes, nanorods and wires (2). In the past decade, electrospun polymer nanofibers have proven to contain many of the unique properties desirable for biotech development. Recent work using electrospun nanofibers covers a wide range of applications, including optical sensors and biosensors, filtration membranes, drug delivery devices, and scaffolding for stem cell growth (3−7).

Electrospinning is a polymer processing technique used to create fibers with diameters ranging from a few nanometers to micrometers (8). The electrospinning process works when a flowing polymer solution is subject to a high electric field. When the repulsive electrostatic force overcomes the surface tension of the polymer solution a stable jet is formed and a membrane-like web of small fibers is emitted onto the ground electrode (9). The use of electrospun nanofibers for chemical sensors using fluorophores has been previously reported. For instance, Samuelson and co-workers have demonstrated that pyrene methanol and hydrolyzed poly[2-(3-thienyl) ethanol butoxy carbonyl-methyl urethane] (H-PURET) can be immobilized to the surface of electrospun membranes for the detection of metal ions (Fe^{3+} and Hg^{2+}), 2,4-dinitrotoluene (DNT), and methyl viologen (MV^{2+}) (10, 11). Tao et al. reported the use of sol−gel chemistry to make porphyrin-doped nanofibrous membranes for the detection of 2,4,6-trinitrotoluene (TNT) vapor (12). A major drawback of these platforms, however, is that they require multiple fabrication steps, resulting in inhomogeneous dispersion of sensing molecules within the membrane and potential fluorescent leakage, and ultimately compromising sensitivity, stability, and reproducibility of the solid-state optical sensors. More recently, Yang et al. demonstrated that secondary porous structures could be added to 9-chloromethylanthracene (9-CMA)-doped cellulose acetate (CA) nanofibers for the detection of MV^{2+} (13). Although Yang's work provided a simple approach to creating secondary pores within the nanofiber, there is still a need for new fluorescent units that demonstrate distinctive FRET properties and better process characteristics, such as improved retention, all of which are important for generating new protein sensors.

Fluorescent dendrimers are highly effective receptors for fluorescent optical sensors for many different target analytes, such as explosives (TNT and DNT) and biomarkers

* Corresponding author. Tel: (951) 827-2702 (Q.C.). E-mail: quan.cheng@ucr.edu (Q.C.); mongkol.s@chula.ac.th(M.S.).
Received for review April 19, 2010 and accepted June 22, 2010
[†] University of California.
[‡] Chulalongkorn University.
DOI: 10.1021/am100345g

Published on Web 06/29/2010

Scheme 1. Schematic Illustration of the Electrospinning Setup, Encapsulation of the Fluorescent Dendrimer, And Deacetytlation Process Used in This Study; Five Water-Soluble Fluorescent Dendritic Compounds (AFD-1, AFD-2, AFD-3, AFD-4, and AFD-5) Composed of Phenylene-Ethynylene Repeating Units Are Illustrated[a]

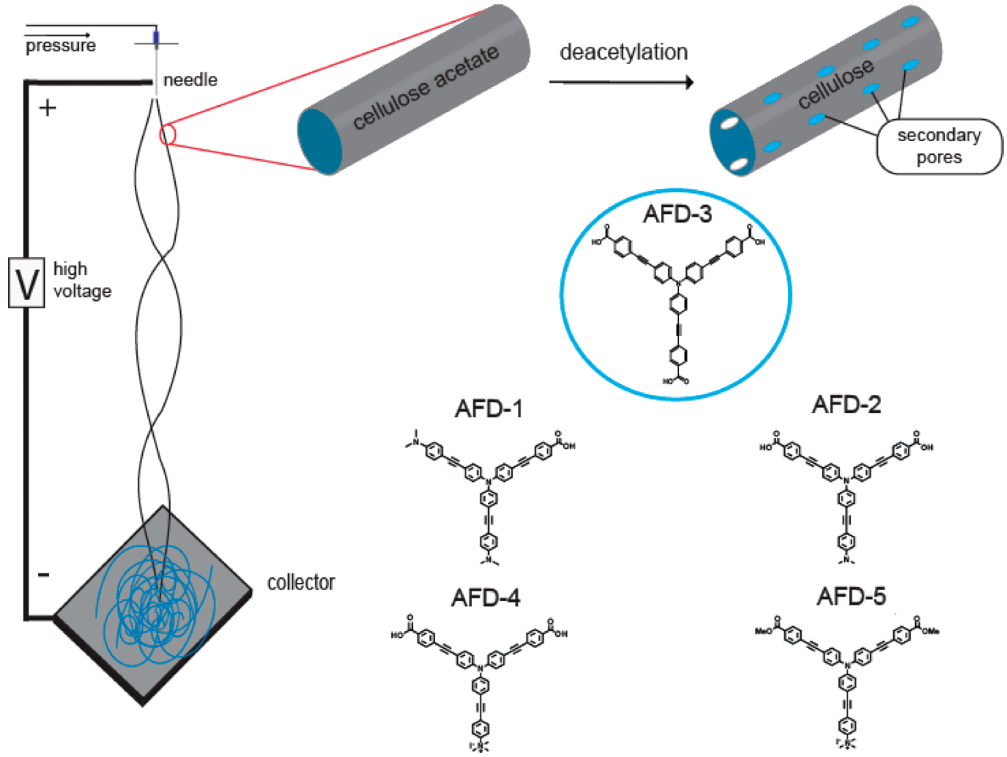

[a] The circled AFD-3 is the fluorescent dye used to dope the CA nanofibers for detection of metalloproteins.

(14−18). In comparison with molecular fluorophores, the numbers of fluorophore units in dendrimers can be controlled by simple synthetic means. This convergent approach allows for more predictable structure-related and fluorescent properties within the sensor. In this work, a diphenylacetylene dendritic compound containing negatively charged peripheral groups is used as an effective bioreceptor. In the past, Thayumanavan and co-workers have utilized dendritic scaffolding to generate fluorescence-based patterns for both metalloprotein and nonmetalloprotein sensing using solution based detection schemes (19−22). The quenching property of their sensor was reported to be caused by the charge density around the protein, as well as quantity and position of the heme within the metalloproteins. Although the use of fluorescent dendrimers for solution-based protein detection exists (19), there is still a lack of research that uses simple approaches to creating reusable solid-state devices that can respond differentially to a variety of proteins. In this work, we report a novel solid-state fluorescent biosensor, using nanofibers, for quantifying proteins in solution. A straightforward top-down in situ electrospinning approach is utilized along with anionic fluorescent dendrimers (AFD) to fabricate a reusable sensor for the detection of low concentrations of metalloproteins via a fluorescence resonance energy transfer (FRET) principle.

2. EXPERIMENTAL SECTION

All chemicals were of the highest analytical grade, purchased from Sigma-Aldrich (Milwaukee, WI) and used without further purification, unless otherwise stated. Milli-Q (>18 MΩ) water was used in the preparation of all buffer solutions. Steady-state fluorescence measurements were performed on a HORIBA FluoroLog spectrofluorometer using the excitation at 370 nm. Fluorescence image analysis was performed on a Leica TCS SP2/UV confocal microscope using the excitation at 364 nm. The scanning electron microscope (SEM) used is a Phillips XL30-FEG. Fiber analysis was performed using Fourier transform infrared (FTIR) spectroscopy on a Equinox 55/S FTIR spectrometer with a Bruker A590 microscope.

CA is used as the host matrix in our nanofiber fabrication because of its chemical resistance, thermal stability, low nonspecific absorption, and capacity to be easily functionalized with recognition elements (23). To further improve the surface area:volume ratio and overall performance a simple deacetylation treatment was used to create specific secondary structures within our electrospun nanofibers. Park and co-workers have demonstrated that secondary porous structures can be inserted into the backbone of electrospun CA fibers by homogeneous deacetylation treatment of CA to cellulose using a practical processing step while at the same time maintaining the nanofiber's physical properties (24−26). This deacetylation treatment is used in our work to generate evenly distributed secondary pores throughout the nanofiber backbone of cellulose to improve the sensing performance. A schematic illustration of the electrospinning

setup, encapsulation of the fluorescent dendrimer, and deacetylation process is shown in Scheme 1.

Five water-soluble fluorescent dendritic compounds (AFD-1, AFD-2, AFD-3, AFD-4, and AFD-5) composed of phenylene-ethynylene repeating units (Scheme 1) were synthesized according to published procedures and screened in solution for the highest visible fluorescence (see the Supporting Information) (27). These dendrimers commonly demonstrated low visible fluorescent emission, but AFD-3 was found to be an exception that gave visibly high fluorescence. The variability of the fluorescent emission among the dendrimers is due to aggregation, which is caused by small differences in the charge distribution among different AFDs.

The electrospinning solution was prepared by dissolving 17% CA and 0.1% AFD-3 (by weight) in 8:1 (v/v) Acetone/H_2O, and then placed into a plastic syringe. A high-voltage DC power supply (Glassman High Voltage Inc. Series EH) was connected to a 25-gauge blunt nose needle attached to the syringe containing the electrospinning solution. The electrospun fibers were collected on a grounded aluminum plate. The CA/AFD-3 solutions were electrospun at a voltage of 21 kV, a tip-to-collector distance of 10 cm, and a solution flow rate of 1.2 mL/h. All of the electrospinning procedures were carried out at 25 °C with a collection time of approximately 90 s. To create secondary porous structures, we deacetylated the CA fibers in a 50 mM NaOH ethanol solution at 25 °C for 24 h, thoroughly rinsed them with water, and then dried them using N_2. The chemical reaction of CA to cellulose was traced by using FT-IR spectroscopy (see the Supporting Information). The characteristic absorption peaks attributed to the vibrations of the acetate group at 1745($\nu_{C=O}$), 1375(ν_{C-CH3}), and 1235 cm^{-1}(νC−O−C) disappeared after deacetylation of CA. An absorption peak at 3500 cm^{-1} (ν_{O-H}) was also observed, indicating successful deacetylation. The FT-IR spectrum obtained after deacetylation agreed with that of pure cellulose fibers.

3. RESULTS AND DISCUSSION

The electrospun fibers exhibited well-defined fibrous morphology without bead formation and good structural stability. An electrospun AFD-3-doped nanofiber nonwoven mat is shown in the SEM image in Figure 1, further illustrating the large surface area:volume ratio formed within the electrospun nonwoven film. The fibers were continuous, uniform, and had a diameter ranging from approximately 400−2000 nm, similar to those reported by Xiang et al. (28). One-dimensional (1D) nanostructures are distributed evenly throughout the electrospun membrane using a simple electrospinning approach. It is assumed that the nanofibers are 3D, because of their inherent porosity created by the deacytelation of CA to cellulose. Consequently, unique secondary porous structures are homogenously distributed throughout the backbone of the nanofibers creating a larger surface area: volume ratio and in-turn substantially improving sensitivity.

The protein sensing properties of the fibers were characterized by monitoring the quenching behaviors of cyto-

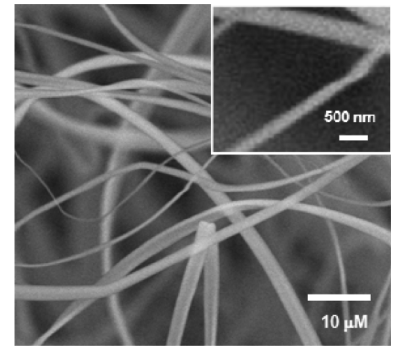

FIGURE 1. SEM image of electrospun AFD-doped deacetylated cellulose fibers (17% CA/0.1% AFD dissolved in 8:1 acetone/water). Inset is a zoomed-in image of the fiber.

chrome c (cyt c), hemoglobin (Hgb), and bovine serum albumin (BSA) as a function of concentration. All proteins were bovine specific, where cyt c is positively charged (pI 10.2−10.7), Hgb is neutral/slightly negative (pI 7.0−7.4), BSA is negatively charged (pI 4.8−4.9), and AFD-3 is negatively charged at physiological pH (29). The fluorescence spectra of the fiber varying with the concentration of cyt c are illustrated in Figure 2a. The fluorescence intensity decreases proportionally with increase in cyt c concentration. Similar behavior was observed with Hgb (Figure 2b). The efficient quenching effects of the metalloproteins, cyt c and Hgb, are primarily due to energy transfer of the imbedded fluorescent dendrimers with the protein as both cyt c and Hgb contain heme portions within the protein. Some of the quenching effect for proteins can be attributed to electron transfer, caused through the electrostatic effects in the binding of the anionic dendrimer to the positive patches of globular proteins. When BSA was used, however, an increase in fluorescence was observed (Figure 2c). The slight increase in local fluorescence of the dendritic fluorophore within the high-surface-area of the nanfibers suggested that the negatively charged BSA proteins reduce the $\pi-\pi$ stacking of the partially dispersed negatively charged dendritic fluorophores through repulsion forces, resulting in an increase in fluorescence (30, 31). It is expected that two main factors contribute to protein detection: (1) the charge distribution density on the proteins surface, and (2) the location of the metalloproteins secondary structure. The intricate nature of the interaction of these two factors should result in protein-dependent patterns allowing for good sensing capabilities.

The fluorescence dynamic quenching sensitivity can be quantified through the measurements with the Stern−Volmer equation (32)

$$\frac{I_0}{I} = 1 + K_{SV}[Q] \qquad (1)$$

where I_0 and I are the fluorescent intensities in the absence and presence of quencher, respectively; K_{sv} is the Stern−Volmer quenching constant, and [Q] is the concentration of quencher. The quenching data are usually presented as plots

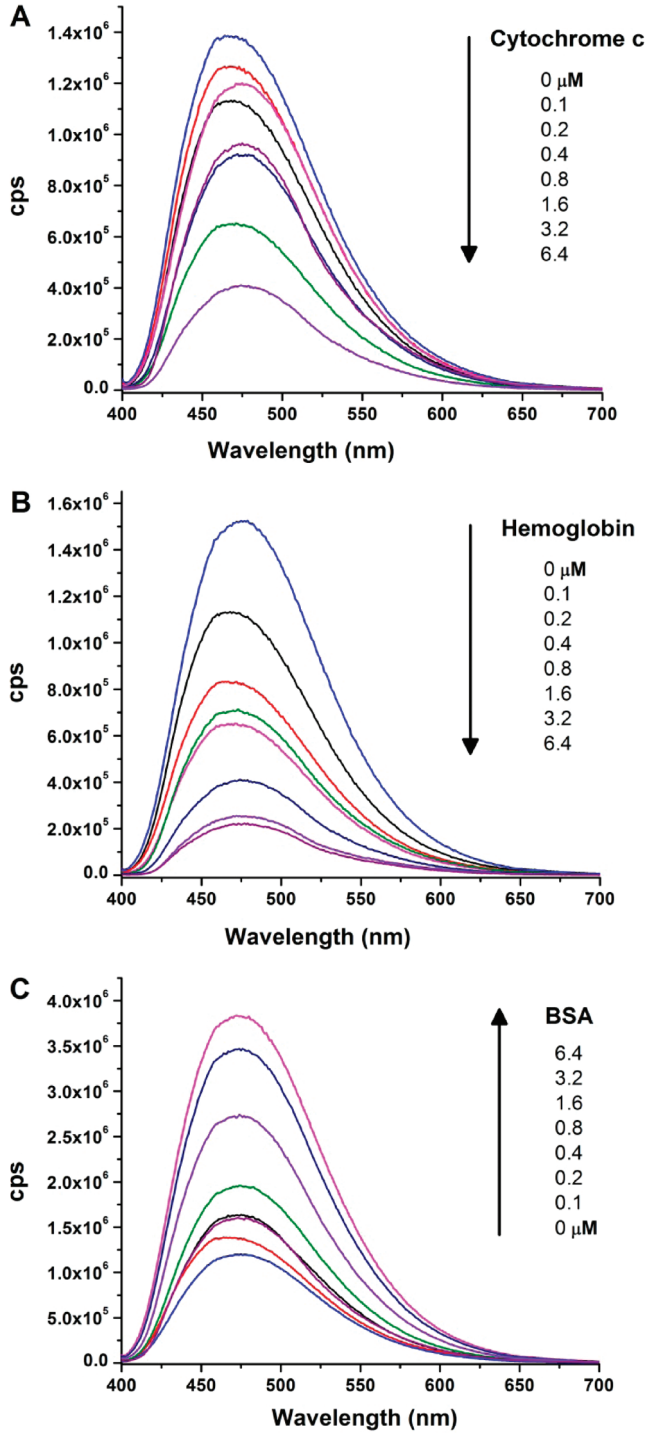

FIGURE 2. Fluorescence emission spectra of the AFD-functionalized nanofibers in response to varied concentrations of (A) cyt c, (B) Hgb, and (C) BSA ($\lambda_{Ex}/\lambda_{Em}$ = 370/475 nm).

of I_0/I versus [Q] with a slope equal to K_{sv}. The higher the K_{sv}, the lower the concentration of quencher is required to quench the fluorescence and thus the greater detection sensitivity.

The Stern–Volmer analysis of the electrospun sensors for cyt c and Hgb is shown in Figure 3. At concentrations between 100 nM and 6.4 μM, a linear relationship between quencher concentration and I_0/I was obtained, showing homogeneous quencher-accessible sites in the electrospun

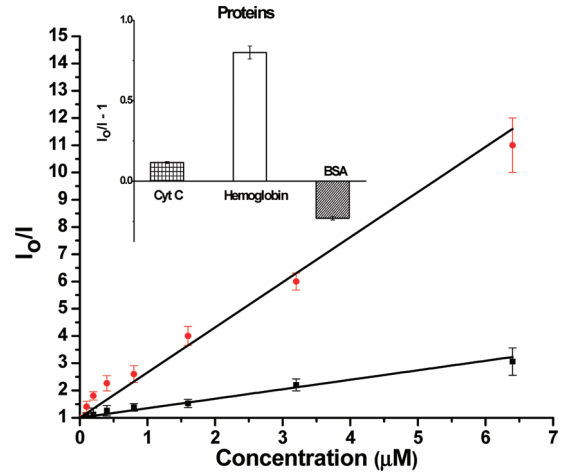

FIGURE 3. Stern–Volmer plots of the nanofibers for cyt c (■) and Hgb (•). Inset: Analyte-dependent pattern for 200 nM of bovine metalloproteins (cyt c, Hgb) and nonmetalloprotein (BSA) in PBS buffer solution (pH 7.4).

fibers under the experimental conditions. The sensitivity, K_{SV}, of the electrospun fibers was found to be 3.4×10^5 and 1.7×10^6 M^{-1} for cyt c and Hgb, respectively. BSA tested under the same experimental conditions demonstrated a small negative linear relationship. The inset in Figure 3 shows the analyte-dependent pattern from the fluorescence intensity changes at 200 nM. Differential responses for different proteins are demonstrated and therefore illustrated anlyte-specific patterns. The results clearly point to an effective approach to the solid-state fabrication of biosensors by embedding selective receptors into electrospun fibers.

The sensitive protein detection was further visualized using a high resolution UV confocal microscope. Figure 4 shows the fluorescence images of the AFD-3-doped cellulose nanofibers before and after incubation with 10 μM cyt c solution for 15 min, further illustrating the remarkable quenching effect of the nanofiber sensors. The fluorescence images before the quenching process indicate the evident fluorescence emission and the uniform dispersion of fluorophores in cellulose, which is beneficial to sensing performance.

The reusability, reproducibility, and stability of the nanofiber material were also investigated. To demonstrate the reusability of the sensor, we immersed the cellulose nanofibers in a 25 μM solution of cyt c for 5 min, and then in a 50 mM NaOH ethanol solution for 15 min followed by rinsing in water and drying in air. The fibers were then reused for sensing the same cyt c solution. Figure 5 demonstrates that the used nanofibers contain similar quenching ability as the pristine fibers. In the tested 5 cycles, the nanofibers exhibited less than 15% loss of fluorescence intensity signal, indicating outstanding reusability. We attribute this to the noncovalent nature of the interaction, which is largely based on the electrostatic interaction between the fluorophore and protein. In fact, that weak binding events and striping process do not denature the core, which allows for excellent sample recovery. The reproducibly of the sensor is reflected by low batch-to-batch variation of 5.3% for the CA/AFD-3 nanofibers using 3 separate measurements produced on different days. For the stability

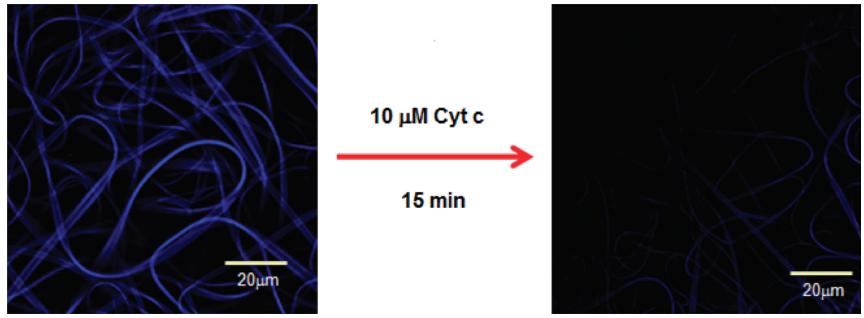

FIGURE 4. Confocal fluorescence images of the electrospun nanofibers before (left) and after (right) incubation in a 10 μM cyt c solution for 15 min.

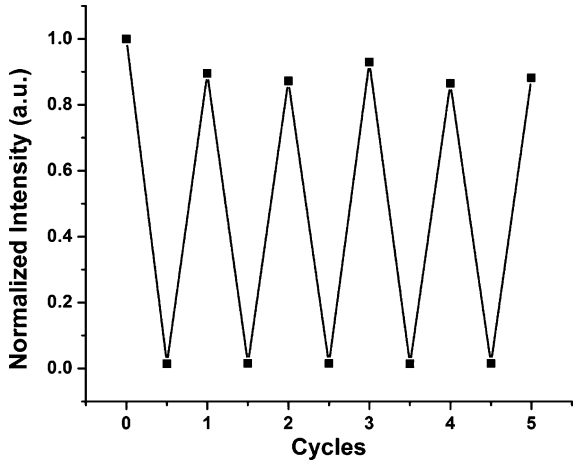

FIGURE 5. Repeated switching of normalized fluorescence emission of the nanofibers for 5 cycles of 25 μM cyt c of quenching/regeneration process. Quenching time: 15 min, regenerated by immersing into 50 mM NaOH ethanol solution for 5 min, PBS buffered solution (pH 7.4) for 5 min and dried with N_2 gas, $\lambda_{Ex}/\lambda_{Em}$ = 370/475 nm.

experiments, we tested the buffer solutions before and after each test and no leakage of the fluorophore were found in the aqueous solutions.

4. CONCLUSIONS

In conclusion, a reusable, solid-state fluorescent biosensor was developed using electrospun nanofibers and anionic dendrimers for quantifying proteins in solution via a FRET mechanism. The selectivity and specificity of the sensor is displayed in the specific response each protein has with the fluorescent fibers. The quenching effect is a result of energy/electron transfer processes between iron containing proteins (i.e., cyt c and Hgb) and the fluorescent core. The increase in fluorescence by the BSA is due to the induced decrease in $\pi-\pi$ stacking of the AFD-3 fluorophore localized on the surface of the nanofibers. A relatively large quenching sensitivity was obtained for AFD-3-doped cellulose nanofibers with respect to Hgb, which is demonstrated with the Stern–Volmer constants. The electrospun doped fibrous material exhibited large surface area due to small diameter and porosity of the nanofibers. This porosity stems from two factors: the deacetylation of CA to cellulose and the disorderly arrangement of fibers onto the substrate. The ability to homogenously embed fluorophores into the core of the fiber allows for better reproducibility, reversibility, and durability of the sensor. Future efforts will focus on exploring a nanofiber sensor array containing different fluorescent dendrimers for the detection and identification of protein targets via distinct fluorescence response patterns.

Acknowledgment. The authors acknowledge financial support from NSF grant CHE-0719224 (Q.C.) and Thailand's National Nanotechnology Center grant NN-B-22-FN9-10-52-06 (M.S.). Images were collected at the Microscopy Core/Center for Plant Cell Biology at the Institute for Integrative Genome Biology at the University of California, Riverside. We thank Jeff Lefler and Craig Graham for the help in the design and construction of the electrospinning setup.

Supporting Information Available: Additional data showing the FTIR spectrum of the deacytelation of the cellulose acetate to cellulose and fluorescence property of dendritic fluorophores in PBS solution (PDF). This material is available free of charge via the Internet at http://pubs.acs.org.

REFERENCES AND NOTES

(1) Ligler, F. S. *Anal. Chem.* **2009**, *81*, 519.
(2) Dzenis, Y. *Science* **2004**, *304*, 1917.
(3) Meinel, A. J.; Kubow, K. E.; Klotzsch, E.; Garcia-Fuentes, M.; Smith, M. L.; Vogel, V.; Merkle, H. P.; Meinel, L. *Biomaterials* **2009**, *30*, 3058.
(4) Luong-Van, E.; Grondahl, L.; Chua, K. N.; Leong, K. W.; Nurcombe, V.; Cool, S. M. *Biomaterials* **2006**, *27*, 2042.
(5) Long, Y. Y.; Chen, H. B.; Yang, Y.; Wang, H. M.; Yang, Y. F.; Li, N.; Li, K. A.; Pei, J.; Liu, F. *Macromolecules* **2009**, *42*, 6501.
(6) Patel, A. C.; Li, S. X.; Yuan, J. M.; Wei, Y. *Nano Lett.* **2006**, *6*, 1042.
(7) Yoon, K.; Kim, K.; Wang, X. F.; Fang, D. F.; Hsiao, B. S.; Chu, B. *Polymer* **2006**, *47*, 2434.
(8) McKee, M. G.; Layman, J. M.; Cashion, M. P.; Long, T. E. *Science* **2006**, *311*, 353.
(9) Huang, Z. M.; Zhang, Y. Z.; Kotaki, M.; Ramakrishna, S. *Compos. Sci. Technol.* **2003**, *63*, 2223.
(10) Wang, X. Y.; Kim, Y. G.; Drew, C.; Ku, B. C.; Kumar, J.; Samuelson, L. A. *Nano Lett.* **2004**, *4*, 331.
(11) Wang, X.; Drew, C.; Soo-Hyoung, L.; Senecal, K. J.; Kumar, J.; Samuelson, L. A. *Nano Lett.* **2002**, *2*, 1273.
(12) Tao, S. Y.; Li, G. T.; Yin, J. X. *J. Mater. Chem.* **2007**, *17*, 2730.
(13) Yang, Y. F.; Fan, X.; Long, Y. Y.; Su, K.; Zou, D. C.; Li, N.; Zhou, J.; Li, K.; Liu, F. *J. Mater. Chem.* **2009**, *19*, 7290.
(14) Guo, M.; Varnavski, O.; Narayanan, A.; Mongin, O.; Majoral, J. P.; Blanchard-Desce, M.; Goodson, T. *J. Phys. Chem. A* **2009**, *113*, 4763.
(15) Wang, D. L.; Gong, X.; Heeger, P. S.; Rininsland, F.; Bazan, G. C.; Heeger, A. J. *Proc. Natl. Acad. Sci. U.S.A.* **2002**, *99*, 49.
(16) Chen, L. H.; McBranch, D. W.; Wang, H. L.; Helgeson, R.; Wudl, F.; Whitten, D. G. *Proc. Natl. Acad. Sci. U.S.A.* **1999**, *96*, 12287.
(17) Woller, E. K.; Walter, E. D.; Morgan, J. R.; Singel, D. J.; Cloninger, M. J. *J. Am. Chem. Soc.* **2003**, *125*, 8820.
(18) Klaikherd, A.; Sandanaraj, B. S.; Vutukuri, D. R.; Thayumanavan, S. *J. Am. Chem. Soc.* **2006**, *128*, 9231.

(19) Jiwpanich, S.; Sandanaraj, B. S.; Thayumanavan, S. *Chem. Commun.* **2009**, 806.
(20) Savariar, E. N.; Ghosh, S.; Gonzalez, D. C.; Thayumanavan, S. *J. Am. Chem. Soc.* **2008**, *130*, 5416.
(21) Sandanaraj, B. S.; Demont, R.; Thayumanavan, S. *J. Am. Chem. Soc.* **2007**, *129*, 3506.
(22) Sandanaraj, B. S.; Demont, R.; Aathimanikandan, S. V.; Savariar, E. N.; Thayumanavan, S. *J. Am. Chem. Soc.* **2006**, *128*, 10686.
(23) Frey, M. W. *Polym. Rev.* **2008**, *48*, 378.
(24) Han, S. O.; Son, W. K.; Youk, J. H.; Park, W. H. *J. Appl. Polym. Sci.* **2008**, *107*, 1954.
(25) Han, S. O.; Youk, J. H.; Min, K. D.; Kang, Y. O.; Park, W. H. *Mater. Lett.* **2008**, *62*, 759.
(26) Son, W. K.; Youk, J. H.; Park, W. H. *Biomacromolecules* **2004**, *5*, 197.
(27) Niamnont, N.; Siripornnoppakhun, W.; Rashatasakhon, P.; Sukwattanasinitt, M. *Org. Lett.* **2009**, *11*, 2768.
(28) Xiang, C. H.; Frey, M. W.; Taylor, A. G.; Rebovich, M. E. *J. Appl. Polym. Sci.* **2007**, *106*, 2363.
(29) Kim, I. B.; Dunkhorst, A.; Bunz, U. H. F. *Langmuir* **2005**, *21*, 7985.
(30) Lavigne, J. J.; Broughton, D. L.; Wilson, J. N.; Erdogan, B.; Bunz, U. H. F. *Macromolecules* **2003**, *36*, 7409.
(31) Turro, N. J.; Lei, X. G.; Ananthapadmanabhan, K. P.; Aronson, M. *Langmuir* **1995**, *11*, 2525.
(32) Lakowicz, J. R. *Principles of Fluorescence Spectroscopy*, 3rd ed.; Springer: New York, 2006.

AM100345G